ORGANOMETALLICS
Article

Organometallics **2011,** *30,* 1269–1277 1269
DOI: 10.1021/om200008t

Intramolecular Insertion of Alkenes into Pd−N Bonds. Effects of Substrate and Ligand Structure on the Reactivity of (P−P)Pd(Ar)[N(Ar^1)(CH$_2$)$_3$CR=CHR′] Complexes

Joshua D. Neukom, Nicholas S. Perch, and John P. Wolfe*

Department of Chemistry, University of Michigan, 930 N. University Avenue, Ann Arbor, Michigan 48109-1055

Received January 6, 2011

Studies on the synthesis and reactivity of a series of (P−P)Pd(Ar)[N(Ar^1)(CH$_2$)$_3$CR=CHR′] complexes **3** are described. These complexes are transformed to observable (P−P)Pd(Ar)[pyrrolidin-2-ylmethyl] complexes **4** via syn insertion of the pendant alkene into the Pd−N bond. Complexes **4** then undergo C−C bond-forming reductive elimination to yield *N*-aryl-2-benzylpyrrolidine derivatives **2**. Kinetic studies indicate the rates of conversion of **3** to **4** and **4** to **2** are within 1 order of magnitude. The effects of phosphine ligand structure, alkene substitution, and the electronic properties of the Ar and Ar^1 groups on reaction rates are reported, as are the results of deuterium isotope effect studies. The mechanism of the aminopalladation step is discussed in detail, and the results of the experiments described in this paper are most consistent with conversion of **3** to **4** via rate-determining ligand displacement followed by fast aminopalladation. These transformations represent rare examples of syn migratory insertion of unactivated alkenes into Pd−N bonds.

Introduction

The syn insertion of alkenes into Pd−N bonds has been implicated as a key step in many useful Pd-catalyzed reactions. For example, Pd-catalyzed alkene carboaminations between γ-aminoalkene derivatives **1** and aryl bromides are believed to involve *syn*-aminopalladation of intermediate palladium(aryl)amido complexes (e.g., **3**), followed by reductive elimination of the resulting (aryl)(pyrroldin-2-ylmethyl)palladium complexes (e.g, **4**) to yield substituted-pyrrolidine products **2** (Scheme 1).[1] The *syn*-aminopalladation step leads to formation of a C−N bond and also leads to the generation of two stereocenters, which are retained in the pyrrolidine products. This mechanistic pathway is also believed to occur in Pd-catalyzed diaminations,[2] oxidative aminations,[3] chloroaminations,[4] aminoacetoxylations,[5] and hetero-Heck transformations.[6,7]

Scheme 1. Pd-Catalyzed Alkene Carboamination

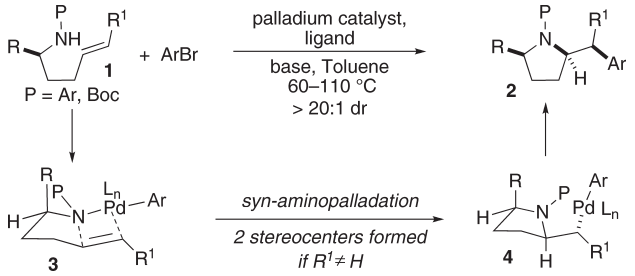

Despite the significance of *syn*-aminopalladation processes, and the influence of this pathway on the stereochemical outcome of synthetically useful reactions, documented unambiguous examples of syn insertions of olefins into late-transition-metal−nitrogen bonds are very rare,[8] and cases involving palladium complexes have only recently been described by our group and Hartwig's group.[9,10] As such, little is known about the effect of palladium amido complex structure on the facility of aminopalladation. However, information

*To whom correspondence should be addressed. E-mail: jpwolfe@umich.edu.

(1) (a) Ney, J. E.; Wolfe, J. P. *J. Am. Chem. Soc.* **2005**, *127*, 8644. (b) Bertrand, M. B.; Neukom, J. D.; Wolfe, J. P. *J. Org. Chem.* **2008**, *73*, 8851. (c) Ney, J. E.; Wolfe, J. P. *Angew. Chem., Int. Ed.* **2004**, *43*, 3605.

(2) (a) Muñiz, K.; Hövelmann, C. H.; Streuff, J. *J. Am. Chem. Soc.* **2008**, *130*, 763. (b) Du, H.; Zhao, B.; Shi, Y. *J. Am. Chem. Soc.* **2007**, *129*, 762.

(3) (a) Liu, G.; Stahl, S. S. *J. Am. Chem. Soc.* **2007**, *129*, 6328. (b) Brice, J. L.; Harang, J. E.; Timokhin, V. I.; Anastasi, N. R.; Stahl, S. S. *J. Am. Chem. Soc.* **2005**, *127*, 2868.

(4) Helaja, J.; Göttlich, R. *Chem. Commun.* **2002**, 720.

(5) Liu, G.; Stahl, S. S. *J. Am. Chem. Soc.* **2006**, *128*, 7179.

(6) Tsutsui, H.; Narasaka, K. *Chem. Lett.* **1999**, 45.

(7) For reviews on metal-catalyzed reactions that involve *syn*-alkene insertion into Pd−N bonds, see: (a) Wolfe, J. P. *Synlett* **2008**, 2913. (b) Minatti, A.; Muñiz, K. *Chem. Soc. Rev.* **2007**, *36*, 1142. (c) Kotov, V.; Scarborough, C. C.; Stahl, S. S. *Inorg. Chem.* **2007**, *46*, 1910.

(8) (a) Villanueva, L. A.; Abboud, K. A.; Boncella, J. M. *Organometallics* **1992**, *11*, 2963. (b) VanderLende, D. D.; Abboud, K. A.; Boncella, J. M. *Inorg. Chem.* **1995**, *34*, 5319. (c) Cowan, R. L.; Trogler, W. C. *J. Am. Chem. Soc.* **1989**, *111*, 4750. (d) Cowan, R. L.; Trogler, W. C. *Organometallics* **1987**, *6*, 2451. (e) Casalnuovo, A. L.; Calabrese, J. C.; Milstein, D. *J. Am. Chem. Soc.* **1988**, *110*, 6738. (f) Zhao, P.; Krug, C.; Hartwig, J. F. *J. Am. Chem. Soc.* **2005**, *127*, 12066.

(9) A portion of the work reported in this article has been previously communicated. See: Neukom, J. D.; Perch, N. S.; Wolfe, J. P. *J. Am. Chem. Soc.* **2010**, *132*, 6276.

(10) For a recent study on intermolecular alkene insertion into Pd−N bonds of palladium amido complexes bearing a cyclometalated phosphine ligand, see: Hanley, P. S.; Markovic, D.; Hartwig, J. F. *J. Am. Chem. Soc.* **2010**, *132*, 6302.

on the relationship between structural features and reactivity could potentially be used to improve the efficiency of catalytic processes or to guide the design of new catalysts for use in challenging reactions or enantioselective transformations.[11]

In this article we describe detailed studies on the synthesis and reactivity of the (P−P)Pd(Ar)[N(Ar^1)(CH$_2$)$_3$CR=CHR′] complexes **3**.[1,12] These complexes undergo syn migratory insertion of the alkene into the Pd−N bond to provide detectable (P−P)Pd(Ar)(pyrrolidin-2-ylmethyl) complexes **4**, which undergo C−C bond-forming reductive elimination to yield *N*-aryl-2-benzylpyrrolidine derivatives **2**. The rates of aminopalladation of **3** and reductive elimination of **4** are influenced by several structural parameters, including the electronic properties of the Ar and Ar^1 groups, the degree of alkene substitution, and the nature of the bis-phosphine ligand. Our experiments suggest the alkene aminopalladation occurs from a four-coordinate complex and illustrate that ligand electronic properties can be tuned to have a positive influence on the rates of both aminopalladation and reductive elimination.

Results

Preliminary Studies on the Synthesis and Reactivity of (dppf)Pd(*p*-C$_6$H$_4$F)[N(*p*-C$_6$H$_4$F)(CH$_2$)$_3$CH=CH$_2$]. Examination of Reaction Rates and Identification of Key Intermediates. In our initial experiments on the intramolecular *syn*-aminopalladation of (aryl)(amido)palladium complexes we elected to examine the generation and reactivity of (dppf)-Pd(*p*-C$_6$H$_4$F)[N(*p*-C$_6$H$_4$F)(CH$_2$)$_3$CH=CH$_2$] (**3a**). The bis-phosphine dppf was selected as the ligand for our preliminary studies, as it provides acceptable yields of *N*-aryl-2-benzylpyrrolidine products in catalytic reactions.[1c,13] In addition, (dppf)Pd(aryl)(amido) complexes have been described in the literature,[14] and the previously reported NMR data could aid in the structural assignment of our complexes. In order to allow for measurement of reaction rates by ^{19}F NMR, we chose to initially study (aryl)(amido)palladium complexes derived from 1-bromo-4-fluorobenzene and *N*-(*p*-fluorophenyl)pent-4-enylamine **1a**.

Prior studies on the synthesis of L$_n$Pd(Ar)(NRR′) complexes suggested that the high reactivity of these species would preclude their isolation in most cases.[14] (Aryl)(amido)palladium complexes are known to undergo relatively facile C−N bond-forming reductive elimination to yield N-arylated amine products, and complexes bearing β-hydrogen atoms can also undergo competing β-hydride elimination. We anticipated the intramolecular alkene aminopalladation of complexes **3** would occur even more rapidly than reductive elimination or β-hydride elimination, as only small amounts of side products resulting from these competing pathways were observed in Pd-catalyzed alkene carboamination reactions.[1c]

Scheme 2. Preliminary Studies

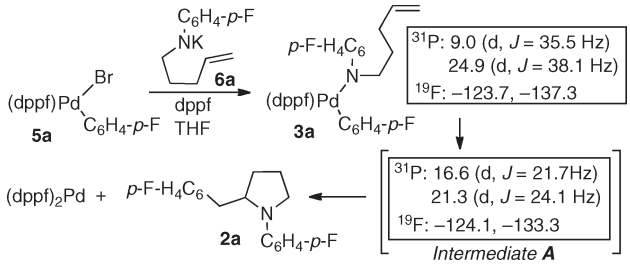

As such, we elected to generate the requisite amido complex **3a** in situ from (dppf)Pd(*p*-C$_6$H$_4$F)(Br) (**5a**)[15] and the potassium anilide salt of *N*-(*p*-fluorophenyl)pent-4-enylamine (**6a**).

In our first series of experiments, a solution of **5a** in THF or THF-d_8 in an NMR tube was treated with **6a** (1.05 equiv) in the presence of 2-fluorotoluene as internal standard and dppf (2 equiv) as a trap for Pd(0) (Scheme 2). Upon mixing, the solution underwent a rapid color change from orange to bright red, and analysis of the mixture by ^{31}P and ^{19}F NMR spectroscopy indicated the starting complex **5a** had been consumed in less than 90 s. The formation of amido complex **3a** was evident by the presence of a pair of doublets at 24.9 ppm (J_{PP} = 38.1 Hz) and 9.0 ppm (J_{PP} = 35.5 Hz) in the ^{31}P NMR spectrum, which are comparable to data previously reported for (dppf)Pd(Ar)[N(Ar^1)(R)] complexes.[14,16] New signals at −123.7 and −137.3 ppm were also observed in the ^{19}F NMR spectrum of **3a**.

Within 2 min amido complex **3a** underwent reaction to generate detectable amounts of a new intermediate complex (**A**), which exhibited ^{19}F NMR resonances at −124.1 and −133.3 ppm and ^{31}P NMR signals at 21.3 ppm (J_{PP} = 24.1 Hz) and 16.6 ppm (J_{PP} = 21.7 Hz). As the conversion of **3a** to **A** proceeded, pyrrolidine **2a** and (dppf)$_2$Pd were generated at a rate that appeared to be roughly comparable to that of the **3a** to **A** transformation. Overall, the conversion of **3a** to **2a** proceeded in 86% NMR yield in 45 min at 24 °C. No additional intermediates on the pathway from **3a** to **2a** were detected, and no side products resulting from β-hydride elimination were observed. Quantitative measurement of reaction kinetics at 24 °C provided a data set consistent with consecutive first-order reactions for the transformation of **3a** to **A** and the transformation of **A** to **2a** (Figures 1, 2). Rate constants were extracted for the two first-order reactions (**3a** to **A**, k_1 = (1.74 ± 0.02) × 10^{-3} s^{-1}; **A** to **2a**, k_2 = (1.36 ± 0.41) × 10^{-3} s^{-1}),[17,18] which occur with rates that are nearly identical. Neither excess dppf nor excess **6a** had an effect on k_1 or k_2.

On the basis of our prior studies on Pd-catalyzed alkene carboamination reactions, the most likely candidates for intermediate **A** are the five-coordinate alkene complex **7a** (Figure 3), which would arise from intramolecular alkene binding of **3a**, or

(11) For enantioselective reactions that are believed to occur via *syn*-aminopalladation see: (a) Mai, D. N.; Wolfe, J. P. *J. Am. Chem. Soc.* **2010**, *132*, 12157.

(12) For a related intramolecular insertion of an unactivated alkene into a Rh−O bond, see: Zhao, P.; Incarvito, C. D.; Hartwig, J. F. *J. Am. Chem. Soc.* **2006**, *128*, 9642.

(13) Dpe-phos provides optimal results in catalytic transformations of *N*-(phenyl)pent-4-enylamine, but this ligand displays somewhat complicated coordination chemistry and can behave as either a cis- or trans-chelating ligand. Moreover, in our hands the preparation of (dppf)Pd(Ar)(Br) complexes proved more straightforward than synthesis of analogous (dpe-phos)Pd(Ar)(Br) complexes.

(14) Yamashita, M.; Cuevas Vicario, J. V.; Hartwig, J. F. *J. Am. Chem. Soc.* **2003**, *125*, 16347.

(15) Ligand definitions: dppf = 1,1-bis(diphenylphosphino)ferrocene; dpp-benzene = 1,2-bis(diphenylphosphino)benzene; dppe = 1,2-bis(diphenylphosphino)ethane; dppp = 1,3-bis(diphenylphosphino)propane; BINAP = 2,2′-bis(diphenylphosphino)-1,1′-binaphthyl; dpe-phos = bis(2-diphenylphosphino)phenyl ether; xantphos = 9,9-dimethyl-4,5-bis(diphenylphosphino)xanthene.

(16) Key data from ref 14 for (dppf)Pd(C$_6$H$_4$-*p*-CF$_3$)[N(Me)(C$_6$H$_4$-*p*-Me)]: ^{31}P NMR (−45 °C) δ 9.3 (br), 24.3 (d, J = 38 Hz).

(17) Emanuel, N. M.; Knorre, D. G. *Chemical Kinetics: Homogeneous Reactions*; Wiley: New York, 1973 (English translation by Kondor, R.; Slutzkin, D.).

(18) Kinetic data are reported as average values for k_1 and k_2 over two or more separate runs.

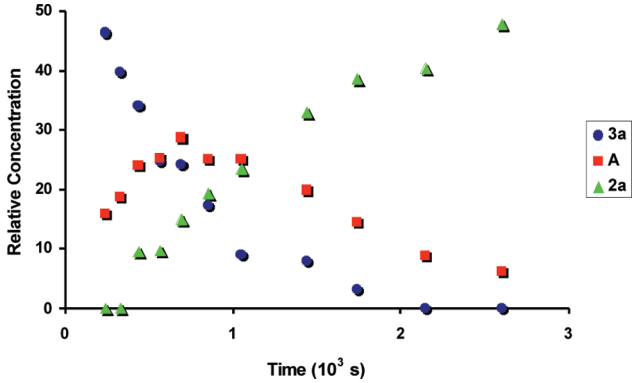

Figure 1. Kinetic plot for the conversion **3a** → **A** → **2a**.

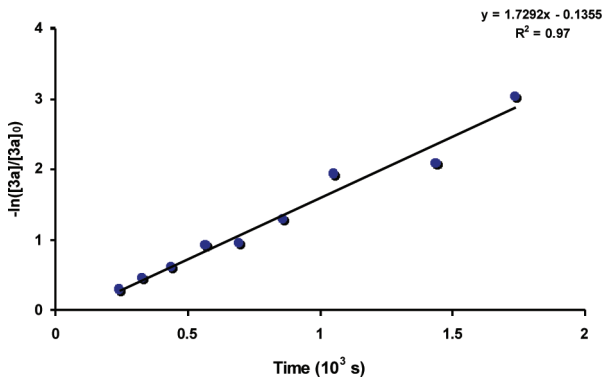

Figure 2. Plot of $-\ln([\mathbf{3a}]/[\mathbf{3a}]_0)$ vs time.

the aryl(alkyl)palladium complex **4a**, which derives from *syn*-aminopalladation of **3a**. In addition, although Pd-catalyzed carboamination reactions have been shown to proceed through aminopalladation pathways,[1] we sought to exclude the possible intermediacy of **8a**, which would result from carbopalladation of **3a**, in the stoichiometric transformation. Unfortunately, the data obtained in our initial experiments could not be used to unambiguously assign the structure of **A**. For example, the ^{1}H NMR alkene signals of **3a** decreased as the reaction proceeded, but this region of the spectrum was sufficiently complicated that the presence of a new alkene-containing intermediate (**7a**) could not be definitively confirmed or refuted. Similarly, the complicated ^{1}H NMR data also did not allow for differentiation of **4a** vs **8a**. We observed that (dppf)Pd(C_6H_4-*p*-F)[CH_2-(cyclopentyl)] (**9**) generated in situ from **5a** and (cyclopentyl)-CH_2MgBr underwent C−C bond-forming reductive elimination in < 5 min at room temperature,[19] which seemed to argue against the intermediacy of **4a**. However, the reductive elimination of **4a** could be significantly slowed relative to **9** due to the inductive electron-withdrawing effect of the nitrogen atom in **4a**.[20] Thus, the identity of intermediate **A** could not be ascertained without additional experimentation.

In order to elucidate the structure of **A**, we prepared and examined the reactivity of ^{13}C-labeled amido complex **3a-^{13}C$_3$**

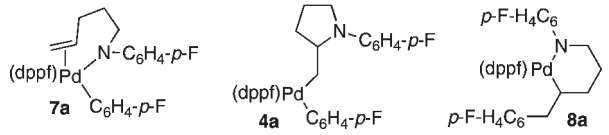

Figure 3. Possible structures of intermediate **A**.

Scheme 3. ^{13}C Labeling Experiments

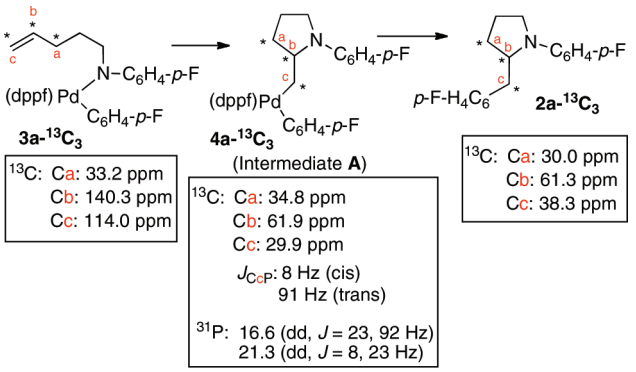

(Scheme 3). Analysis of the reaction by ^{13}C and ^{31}P NMR indicated that intermediate **A** is the aryl(alkyl)palladium complex **4a**. The chemical shifts of the labeled carbon atoms in **A** were not consistent with an alkene, and the chemical shift of C_b indicated it was located adjacent to a heteroatom. Thus, these data ruled out the possible intermediacy of **7a** and **8a**.[21] Moreover, the ^{31}P chemical shifts, coupling constants, and J_{CP} values for **A**/**4a** correlate well with data for (dppf)Pd(Ph)(Me).[19,22]

Effects of Palladium−Amido Complex Structure on Reactivity. Following our initial experiments on the reactivity of complex **3a**, we sought to probe the effects of N-aryl group structure, Pd-aryl group structure, and ligand structure on the rate of the alkene aminopalladation process. To this end, a series of (bis-phosphine)Pd(Ar)(Br) complexes were prepared using standard routes[23] and were treated with potassium salts of *N*-(aryl)pent-4-enylamine derivatives in a manner analogous to that described in Scheme 2. In all cases the amido complexes (**3a**−**k**) were generated in < 2 min at 24 °C and were characterized by diagnostic ^{31}P NMR signals with chemical shifts close to those observed for **3a**.[24] Reactions were allowed to proceed at room temperature, and kinetic data were collected by ^{19}F NMR spectroscopy. Rate constants for k_1 (conversion of **3** to **4**) and for k_2 (conversion of **4** to **2**) were then determined as outlined above[17,18] and are provided in Table 1.

Hammett plots were constructed from the data shown in Table 1. Clear trends were observed in transformations of complexes **3a**−**f** bearing various N-aryl substituents, and linear plots of $\log(k_R/k_H)$ were obtained for both steps in the conversion of **3a**−**f** to **2a**−**f** (Figure 4). Best fits were

(19) Brown has demonstrated that (dppf)Pd(Ph)(Me) undergoes C−C bond-forming reductive elimination with a rate constant of 1.32×10^{-3} s^{-1} at 0 °C. See: Brown, J. M.; Guiry, P. J. *Inorg. Chim. Acta* **1994**, *220*, 249.

(20) Prior studies have indicated that relative rates of C−C bond forming reductive elimination from $L_2Pd(Ar)(CH_2R)$ complexes dramatically decrease as the R group electron-withdrawing group ability increases. See: Culkin, D. A.; Hartwig, J. F. *Organometallics* **2004**, *23*, 3398.

(21) See the Supporting Information for a detailed description of the structural assignment of **4a**.

(22) Key data from ref 19 for (dppf)Pd(Ph)(Me): ^{31}P NMR δ 17.8 (d, J = 23 Hz), 21.3 (d, J = 23 Hz); ^{13}C NMR J_{CP} = 9 Hz (cis), 97 Hz (trans).

(23) (a) Widenhoefer, R. A.; Zhong, H. A.; Buchwald, S. L. *J. Am. Chem. Soc.* **1997**, *119*, 6787. (b) Driver, M. S.; Hartwig, J. F. *J. Am. Chem. Soc.* **1997**, *119*, 8232. (c) Zuideveld, M. Z.; Swennenhuis, B. H. G.; Boele, M. D. K.; Guari, Y.; van Strijdonck, G. P. F.; Reek, J. N. H.; Kamer, P. C. J.; Goubitz, K.; Fraanje, J.; Lutz, M.; Spek, A. L.; van Leeuwen, P. W. N. M. *Dalton Trans.* **2002**, 2308.

(24) See the Supporting Information for complete experimental details and characterization data.

Table 1. Effect of N-Aryl Group and Pd-Aryl Group on Reaction Rates[a]

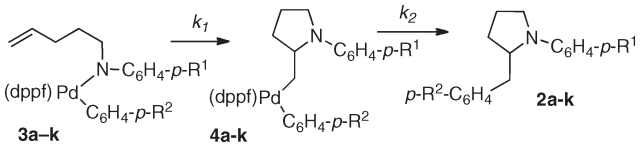

Starting Complex	Intermediate Complex	Product	R^1	R^2	k_1 ($10^{-3}s^{-1}$)	k_2 ($10^{-3}s^{-1}$)
3b	**4b**	**2b**	^{t}Bu	F	5.59 ± 0.46	2.64 ± 0.45
3c	**4c**	**2c**	OMe	F	4.45 ± 0.70	2.18 ± 0.38
3d	**4d**	**2d**	H	F	2.44 ± 0.12	1.88 ± 0.07
3a	**4a**	**2a**	F	F	1.74 ± 0.02	1.36 ± 0.41
3e	**4e**	**2e**	Cl	F	0.56 ± 0.02	0.90 ± 0.02
3f	**4f**	**2f**	CN	F	0.042 ± 0.006	0.42 ± 0.14
3g	**4g**	**2g**	F	^{t}Bu	3.55 ± 0.08	4.08 ± 0.52
3h	**4h**	**2h**	F	OMe	4.03 ± 1.15	2.64 ± 1.13
3i	**4i**	**2i**	F	H	4.55 ± 0.49	9.00 ± 1.33
3j	–	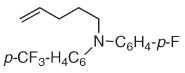	F	CF_3	–[b]	–[b]
3k	–	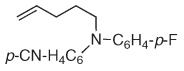	F	CN	–[b]	–[b]

[a] Conditions: all reactions were conducted in NMR tubes with [**3**] = 6.26 mM, [dppf] = 12.6 mM, [2-fluorotoluene] = 11.8 mM (internal standard), THF, 24 °C. All values for k_1 and k_2 are the averages obtained over two or more runs. [b] C–N bond-forming reductive elimination from **3** to provide the corresponding *N*-(C_6H_4-*p*-F)-*N*-(C_6H_4-*p*-R^2)-pent-4-enylamine was the predominant reaction pathway observed.

obtained using the Hammett σ_p parameters, which gave $\rho = -2.5 \pm 0.2$ for step 1 (**3** to **4**) and $\rho = -0.92 \pm 0.06$ for step 2 (**4** to **2**). The increased reactivity of complexes bearing electron-rich N-aryl groups is consistent with trends previously reported by Hartwig for alkene insertion reactions of cyclometalated [^{t}Bu$_2$PCH$_2$C$_6$H$_4$]Pd(NAr$_2$) complexes.[10]

A similar analysis of data obtained in reactions of *N*-(*p*-fluorophenyl)pentenylamine derived complexes **3a**,**g**–**k** bearing various R^2 groups failed to provide clear trends. Hammett plots derived from this series of experiments were nonlinear (Figure 5), although all values of k_1 for this series were within a factor of 2.5 of each other and all values of k_2 for this series were within a factor of 7 of each other. As such, although the precise effect of Pd-aryl substituent on reactivity is unclear, it appears to be relatively small. We were unable to obtain k_1 and k_2 values for reactions of complexes derived from electron-poor aryl bromides (R = CN, CF_3), as these complexes underwent rapid C–N bond-forming reductive elimination (full conversion was observed in < 1 min at room temperature) to yield *N*-(*p*-fluorophenyl)-*N*-(C_6H_4-*p*-R^2)pent-4-enylamines, rather than the desired aminopalladation to afford **4**.

The steric and electronic properties of the bis-phosphine ligand also had a significant influence on reactivity in the conversion of **3l**–**r** to **2e**. As shown in Table 2, the fastest transformations were observed with wide bite angle ligands *N*-methyl-nixantphos[25] and xantphos.[15] Amido complexes **3q**,**r**, bearing these ligands, were rapidly converted to pyrrolidine **2e** at 24 °C with rates too fast to accurately measure; both reactions proceeded to completion in < 1 min. In contrast, complexes **3l**–**o**, bearing ligands with relatively small bite angles, failed to undergo the desired transformation. Complexes **3m**,**o** did not react at temperatures up to 60 °C, and complexes **3l**,**n** decomposed to afford complex mixtures of products.[26] The dpe-phos complex **3p** was transformed to **2e** with an observed rate constant of 0.686×10^{-3} s^{-1}; no intermediate complex **4** was detected during this reaction.

The effect of ligand electronic properties on reaction rates was examined through comparison of complexes bearing differently substituted dppf-derived ligands. As shown in Table 3, the presence of para-electron-withdrawing trifluoromethyl groups on the P–Ar substituents in complex **3s** led to acceleration of both steps of the transformation to **2d** relative to the analogous reaction of parent dppf complex **3d**. In contrast, decreased rates were observed for both steps in the conversion of complex **3t** bearing para-electron-donating methoxy groups to **2d**.

(25) nixantphos = 4,6-bis(diphenylphosphino)phenoxazine. An N-methylated derivative of nixantphos was employed in these studies to avoid acid/base side reactions between the ligand and the potassium *N*-arylamide salts. The bite angle of this ligand is estimated to be similar to that for *N*-benzyl nixantphos. See: Kamer, P. C. J.; van Leeuwen, P. W. N. M.; Reek, J. N. H. *Acc. Chem. Res.* **2001**, *34*, 895–904.

(26) Hartwig has previously observed that (dppe)Pd(Ph)[N(*p*-tol)$_2$] decomposes to afford vinyldiphenylphosphine.[23b]

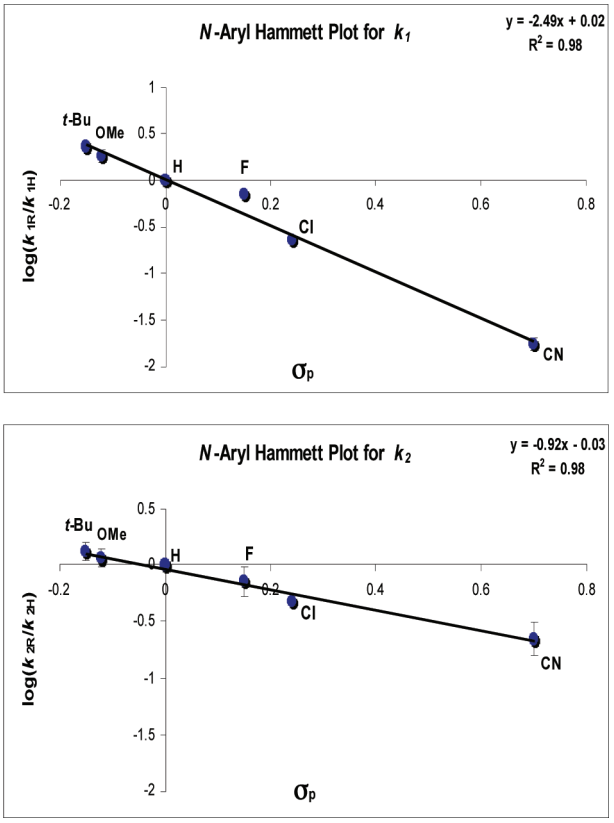

Figure 4. Hammett correlations for the N-aryl group.

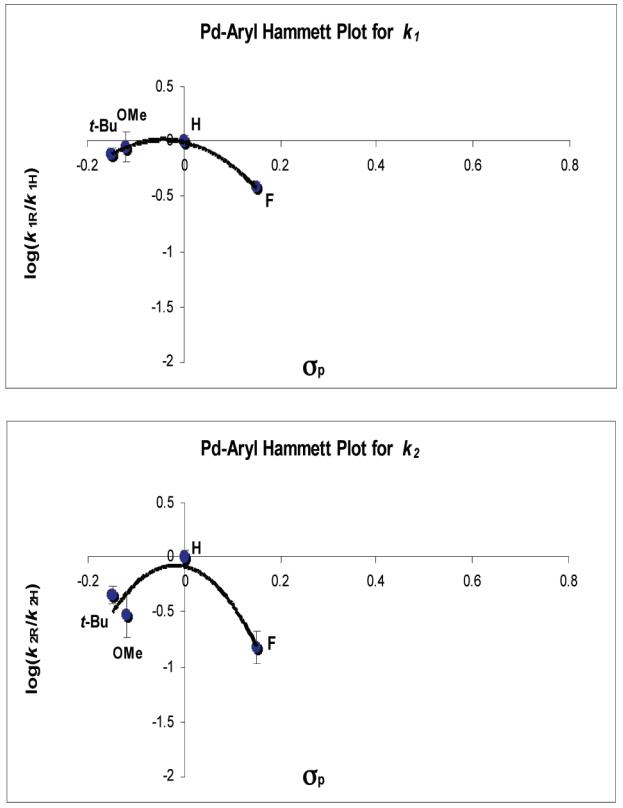

Figure 5. Hammett correlation for Pd-aryl group.

Determination of Activation Parameters. The experiments outlined above indicated that the presence of electron-withdrawing substituents on the N-aryl group decreased the rate of both steps in the conversion of **3** to **2**. Given this information, we elected to examine the activation parameters for this transformation using a complex bearing an electron-poor amido group, which would react at a sufficiently slow rate as to allow for collection of data across a reasonable range of temperatures. Thus, the activation parameters for the conversion of amido complex **3f** to **2f** (by way of **4f**) were determined by Eyring plot analysis over a temperature range of 25−60 °C (Scheme 4).[27] For the conversion of **3f** to **4f** $\Delta H^{\ddagger} = 24.8 \pm 0.6$ kcal/mol and $\Delta S^{\ddagger} = 4.6 \pm 1.8$ eu. For the reductive elimination of **2f** from **4f** $\Delta H^{\ddagger} = 23.3 \pm 0.8$ kcal/mol and $\Delta S^{\ddagger} = 4.6 \pm 2.5$ eu. The reaction enthalpies are comparable to those observed for insertion of alkenes into late-metal−carbon bonds[28a−c] and for C−C bond-forming reductive elimination processes.[28d]

Scheme 4. Activation Parameters

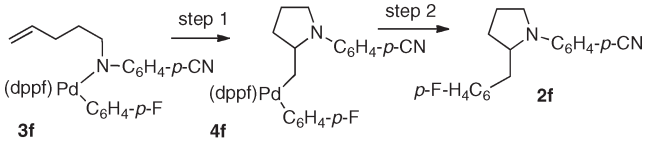

Step 1: $\Delta H^{\ddagger} = 24.8 \pm 0.6$ kcal/mol, $\Delta S^{\ddagger} = 4.6 \pm 1.8$ eu
Step 2: $\Delta H^{\ddagger} = 23.3 \pm 0.8$ kcal/mol, $\Delta S^{\ddagger} = 4.6 \pm 2.5$ eu

Stereochemistry of Alkene Aminopalladation and Deuterium Isotope Effects. The stereochemistry of the aminopalladation reaction was determined through the reaction of deuterated amido complex **3u**. As shown in eq 1, this complex was cleanly transformed to pyrrolidine **2u** with net syn addition of the aryl group and the N atom across the C−C double bond. This supports a mechanism involving syn migratory insertion of the alkene into the Pd−N bond, rather than amide dissociation, alkene coordination, and outer-sphere attack of the pendant nucleophile. This result is also consistent with the stereochemical outcome of Pd-catalyzed carboamination reactions between γ-aminoalkene derivatives and aryl bromides.[1]

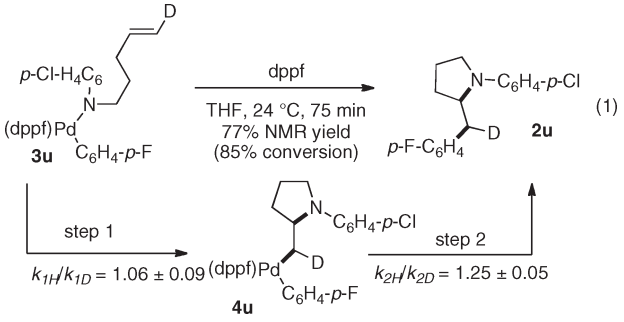

Kinetic measurements were acquired for the two-step conversion of **3u** to **2u** ($k_1 = (0.528 \pm 0.041) \times 10^{-3}$ s^{-1}; $k_2 = (0.701 \pm 0.023) \times 10^{-3}$ s^{-1}) and were compared to values obtained for the analogous nondeuterated complex **3e**. This comparison indicated no significant isotope effect for step 1

(27) The *N*-(C_6H_4-*p*-CN) derivative **3f** was employed for these studies, as it reacted at a slower rate than **3a**, which simplified experimental setup and allowed for rates to be measured over a range of temperatures above room temperature.

(28) (a) Perch, N. S.; Widenhoefer, R. A. *J. Am. Chem. Soc.* **2004**, *126*, 6332. (b) Rix, F. C.; Brookhart, M. *J. Am. Chem. Soc.* **1995**, *117*, 1137. (c) Ermer, S. P.; Struck, G. E.; Bitler, S. P.; Richards, R.; Bau, R.; Flood, T. C. *Organometallics* **1993**, *12*, 2634. (d) Moravskiy, A.; Stille, J. K. *J. Am. Chem. Soc.* **1981**, *103*, 4182.

Table 2. Effect of Ligand Bite Angle on Reactivity[a]

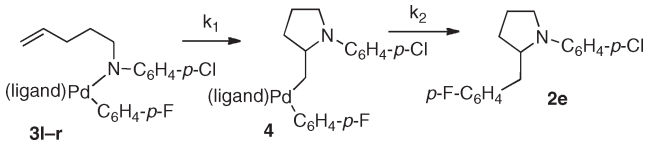

starting complex	intermediate complex	ligand	bite angle (deg)	result
3l	not obsd	dppe	86	dec of complex[b]
3m	not obsd	dpp-benzene	87	no reacn[c]
3n	not obsd	dppp	91	dec of complex[b]
3o	not obsd	(±)-BINAP	93	no reacn[c]
3e	**4e**	dppf	99	$k_1 = (0.56 \pm 0.02) \times 10^{-3}\ s^{-1}$; $k_2 = (0.90 \pm 0.02) \times 10^{-3}\ s^{-1}$
3p	not obsd	dpe-phos	104	$k_{obs} = 0.686 \times 10^{-3}\ s^{-1}$[d]
3q	not obsd	xantphos	108	too fast to measure[e]
3r	not obsd	nixantphos-Me	114	too fast to measure[e]

[a] Conditions: all reactions were conducted in NMR tubes with [**3**] = 6.26 mM, [ligand] = 12.6 mM, [2-fluorotoluene] = 11.8 mM (internal standard), THF, 24 °C. All values for k_1 and k_2 are the averages obtained over two or more runs. [b] Decomposition to afford a complex mixture of products was observed. The expected pyrrolidine **2e** was not detected in significant amounts. [c] No reaction was observed at temperatures up to 60 °C. [d] No intermediate was detected in this reaction. [e] Complete conversion to **2e** was observed within 1 min of mixing **3q**,**r** and the potassium *N*-arylamide salt.

Table 3. Ligand Electronic Effects[a]

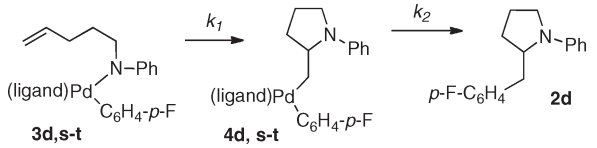

starting complex	intermediate complex	ligand	k_1 ($10^{-3}\ s^{-1}$)	k_2 ($10^{-3}\ s^{-1}$)
3s	**4s**	dppf-*p*-CF_3	4.08 ± 0.03	14.6 ± 2.4
3d	**4d**	dppf	2.44 ± 0.12	1.88 ± 0.07
3t	**4t**	dppf-*p*-OMe	0.77 ± 0.01	0.59 ± 0.20

[a] Conditions: all reactions were conducted in NMR tubes with [**3**] = 6.26 mM, [ligand] = 12.6 mM, [2-fluorotoluene] = 11.8 mM (internal standard), THF, 24 °C. All values for k_1 and k_2 are the averages obtained over two or more runs.

of the transformation (k_{1H}/k_{1D} = 1.06 ± 0.09), but a small isotope effect was observed for the reductive elimination (step 2, k_{2H}/k_{2D} = 1.25 ± 0.05). Related experiments conducted with substrate **3v**, which contains a deuterium atom at the internal alkene carbon, indicated no significant isotope effect (eq 2).

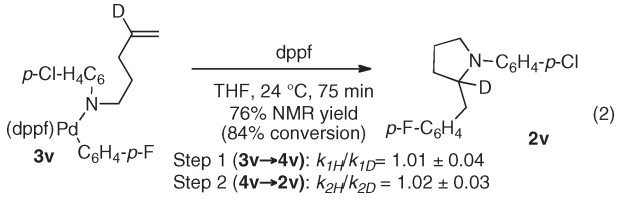

(2)

Effect of Alkene Substitution on Reactivity. In order to probe the effect of alkene substitution on reactivity, complexes **3w**−**y**, bearing 1,1- or 1,2-disubstituted alkenes, were prepared in a manner analogous to that for the amido complexes described above. As shown in Table 4, complex **3w**, which contains a substituent at the internal alkene carbon, undergoes aminopalladation to give intermediate **4w** at a rate that is 10-fold slower than for the analogous conversion of unsubstituted derivative **3d** to **4d**. However, the rate of reductive elimination from intermediate **4w** to yield **2w** is comparable to that for the transformation of **4d** to **2d**. Complexes **3x**,**y** failed to undergo aminopalladation at temperatures up to 60 °C.

Discussion

Plausible Mechanistic Scenarios for the Conversion of Amido Complexes 3 to (Aryl)(pyrrolidin-2-ylmethyl)palladium Complexes 4. The conversion of (bis-phosphine)Pd(Ar)[N-(Ar^1)$(CH_2)_3$C(R)=C(R)(R′)] complexes **3** to (bis-phosphine)Pd(Ar)(pyrrolidin-2-ylmethyl) complexes **4** presumably does not occur via a single step but instead likely involves (a) intramolecular coordination of the alkene to palladium and (b) *syn*-aminopalladation. As such, the conversion of **3** to **4** could potentially proceed through four different reasonable pathways (Scheme 5). Two scenarios would involve *syn*-aminopalladation from the five-coordinate complex **7**. The first would entail rate-limiting alkene coordination of **3** to provide **7**, which could then undergo rapid aminopalladation to afford **4** (path A). Alternatively, fast and reversible intramolecular alkene coordination of **3** would yield **7**, which could undergo rate-limiting aminopalladation to **4** (path B).

Two other possibilities would involve ligand substitution of alkene for one arm of the chelating bis-phosphine ligand to give four-coordinate alkene complex **10** (presumably via an associative mechanism; **7** would be a transient intermediate en route to **10**).[29] One of these pathways (path C) would proceed via rate-limiting associative substitution of **3** to give **10**, followed by fast aminopalladation of **10** to yield **4**. Finally, fast and reversible associative ligand substitution of **3** to **10** followed by rate-limiting aminopalladation from **10** to **4** is also a reasonable possibility (path D).

(29) Ligand substitution reactions of d^8-Pd(II) complexes generally occur via associative pathways. See: (a) Qian, H.; Widenhoefer, R. A. *J. Am. Chem. Soc.* **2003**, *125*, 2056. (b) Shultz, L. H.; Tempel, D. J.; Brookhart, M. *J. Am. Chem. Soc.* **2001**, *123*, 11539and references cited therein. For rare exceptions, which involve very large, sterically bulky ligands, see: (c) Bartolome, C.; Espinet, P.; Martin-Alvarez, J. M; Villafane, F. *Eur. J. Inorg. Chem.* **2004**, 2326. (d) Louie, J.; Hartwig, J. F. *J. Am. Chem. Soc.* **1995**, *117*, 11598.

Table 4. Alkene Substituent Effects[a]

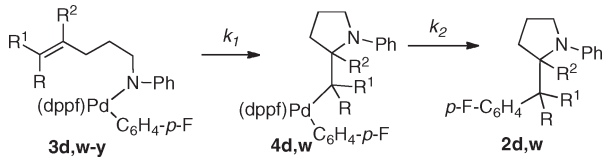

starting complex	intermediate complex	product	R	R^1	R^2	k_1 (10^{-3} s^{-1})	k_2 (10^{-3} s^{-1})
3d	**4d**	**2d**	H	H	H	2.44 ± 0.12	1.88 ± 0.07
3w	**4w**	**2w**	H	H	Me	0.25 ± 0.09	1.58 ± 0.16
3x	not obsd		Me	H	H	[b]	[b]
3y	not obsd		H	Me	H	[b]	[b]

[a] Conditions: all reactions were conducted in NMR tubes with [**3**] = 6.26 mM, [dppf] = 12.6 mM, [2-fluorotoluene] = 11.8 mM (internal standard), THF, 24 °C. All values for k_1 and k_2 are the averages obtained over two or more runs. [b] No reaction was observed up to 60 °C.

As shown in Scheme 5, paths B and D for the conversion of **3** to **4** both involve rapid formation of an alkene-bound complex (**7** or **10**) followed by rate-limiting aminopalladation (from either **7** or **10**). The fact that neither **7** nor **10** is a detectable intermediate argues against paths B and D but cannot be used to rule out these pathways, as it is possible the equilibrium between **3** and **7** or **3** and **10** is fast but lies far to the left, favoring **3**. *In contrast, the results obtained in reactions with deuterated substrates **3u**,**v** provide good evidence that neither path B nor path D is in operation.*[30] The transformations of **7** to **4** and **10** to **4** both involve rehybridization of the alkene carbon atoms from sp^2 to sp^3. As such, if this step were rate limiting, a significant deuterium isotope effect should be observed at both alkene carbon atoms. However, the conversions of deuterated complexes **3u**,**v** to **4u**,**v** proceed at the same rate as the transformation of all-protio complex **3e** to **4e**. Finally, the observed effect of ligand bite angle on reaction rate (Table 2) provides additional evidence against path D, as the bite angle should not influence the rate of aminopalldation from **10** to **4** if the ligand is not bound to the metal by both phosphine groups in the rate-determining step.[31]

Paths A and C both involve rate-limiting alkene coordination to the metal center but differ in the nature of the intermediate complex that undergoes aminopalladation. In path A, aminopalladation would occur directly from the five-coordinate intermediate **7**, whereas path C involves substitution of alkene for phosphine followed by insertion from four-coordinate complex **10**. *Several pieces of evidence indicate that the mechanism of conversion of **3** to **4** does not proceed via path A.* First of all, the positive entropy values measured for the conversion of **3f** to **4f** suggest that path A is not operating, as the conversion of **3** to **7** should have a fairly large negative entropy of activation due to the increase in organization in the transition state between complex **3** with a single chelate (P−P) and **7**, which contains two chelates (P−P and alkene−N). In contrast, the measured entropy of +4.6 eu is consistent with the conversion of **3** to **10** via intermediate **7** (path C), as monochelated complex **10** is less ordered than doubly chelated complex **7**.

The effect of ligand and amine properties on reaction rate can also be used to differentiate between paths A and C. If transformations proceed via path C, the reaction rate should be strongly influenced by factors that favor phosphine displacement.[32] In contrast, the rate of reactions that proceed by way of path A should be insensitive to factors that favor ligand substitution and instead should only be affected by parameters that influence initial alkene binding to the metal. The effect of phosphine ligand properties on reaction rate is most consistent with reaction via path C. As illustrated in Scheme 4, complex **3s**, which contains electron-withdrawing p-CF_3-C_6H_4 groups on the phosphines, reacts ca. 5 times faster than the related complex **3t**, which bears p-MeO-C_6H_4 phosphine substituents. The displacement of one arm of the electron-poor p-CF_3-dppf ligand should be more facile than for the relatively electron rich p-MeO-dppf ligand. In addition, although we were unable to obtain quantitative rate data for ligands with very large or very small bite angles, qualitatively it is clear that the transformation is facilitated by wide bite angle ligands and impeded by ligands with small bite angles. This effect is also consistent with rate-limiting associative ligand substitution (path C).[33]

The reactions of complexes bearing electron-rich N-aryl groups are considerably faster than those bearing electron-poor N-aryl groups. For example, the conversion of complexes **3b**,**c**, which contain electron-donating p-^{t}Bu and p-OMe groups on the N-aryl moiety, to **4b**,**c** is 2 orders of magnitude faster than the conversion of **3f** to **4f** (N-aryl = p-CN-C_6H_4). This electronic effect also suggests that the conversion of **3** to **4** proceeds via path C rather than path A. The electron-rich amido groups should increase the electron density of the metal center, which should in turn increase the ease of phosphine displacement. In contrast, if path A were operating, coordination of the relatively electron-rich alkene should be facilitated by a less electron-rich, more Lewis acidic metal center,[34,35] and rates should be faster with relatively electron-poor N-aryl groups.

(30) Prior studies by Hartwig have shown that cyclometalated four-coordinate [^{t}Bu$_2$PCH$_2$C$_6$H$_4$]Pd(NAr$_2$)(ethylene) complexes undergo very fast insertion of the alkene into the Pd−N bond at temperatures as low as −40 °C.[10]

(31) Although the wide-bite-angle ligands dpe-phos, xantphos, and *N*-Me-nixantphos are more electron rich than dppf, the trends observed with para-substituted dppf derivatives (complexes **3s**,**t**) suggest that the large bite angle is responsible for the rate enhancement rather than electronic properties. The electron-rich complex **3t** reacts at only a slightly slower rate than **3s**. In addition, dpe-phos and xantphos have similar electronic properties, but the complexes bearing these ligands have considerably different reactivities.

(32) The lability of a chelating ligand has previously been observed to influence the rate of carbopalladation in (L−L)Pd(Me)[PPh$_2$(C$_6$H$_4$-*o*-CH=CH$_2$)] complexes. See: Cavell, K. J.; Jin, H. *J. Chem. Soc., Dalton Trans.* **1995**, 4081.

(33) Delis, J. G. P.; Groen, J. H.; Vrieze, K.; van Leeuwen, P. W. N. M. *Organometallics* **1997**, *16*, 551.

(34) Tanaka, D.; Romeril, S. P.; Myers, A. G. *J. Am. Chem. Soc.* **2005**, *127*, 10323.

(35) The opposite trend has been observed in reactions between cationic methylpalladium complexes and electron-poor alkenes. This effect has been ascribed to the influence of π back-bonding interactions between a relatively electron rich metal center and the electron-poor alkene. See: Wu, F.; Jordan, R. F. *Organometallics* **2006**, *25*, 5631–5637.

Scheme 5. Possible Mechanistic Pathways for Conversion of 3 to 4

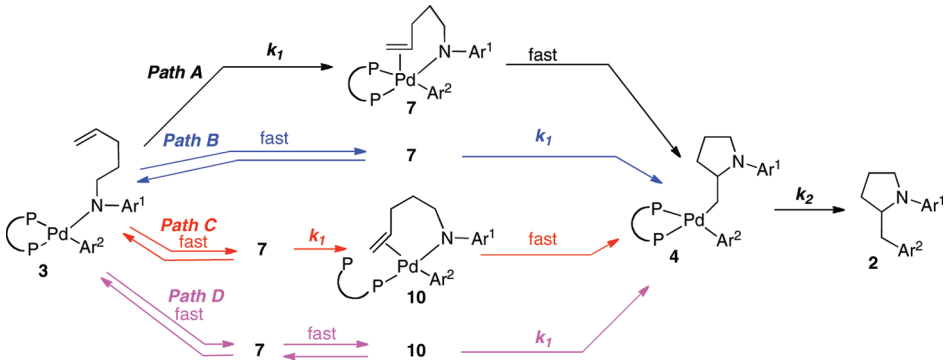

No clear trend was observed for the influence of Pd-aryl group electronics on the rate of conversion of **3** to **4**. As such, these data cannot be used to refute any of the possible mechanistic pathways. The origin of these electronic effects is unclear, but the differences in relative rates of aminopalladation for complexes **3a**,**g**−**i** are small (within a factor of ca. 2). However, our data do indicate that the rate of C−N bond-forming reductive elimination dramatically increases relative to the rate of aminopalladation in complexes **3j**,**k**, which contain strong electron-withdrawing substituents on the Pd-Ar group.

Influence of Structural Features on Carbon−Carbon Bond-Forming Reductive Elimination of 4 To Afford 2. The rate of C−C bond-forming reductive elimination from (dppf)Pd(Ar)(pyrrolidin-2-ylmethyl) complexes **4** is also affected by the structural features of the complexes. For example, the electronic properties of the N-aryl group have a significant influence on this transformation, as complexes **4** bearing electron-rich N-aryl groups undergo reductive elimination 5 times faster than electron-poor derivatives. In addition, the rate of reductive elimination of the (dppf)Pd(Ar)(pyrrolidine-2-ylmethyl) complexes is considerably slower than the analogous reaction of the (dppf)Pd(Ar)(alkyl) derivative (dppf)Pd(C_6H_4-*p*-F)[CH_2(cyclopentyl)] (**9**). These trends are likely due to inductive effects that slow the relative rate of reductive elimination as the electron-withdrawing power of the nitrogen atom increases in derivatives of **4**.[20] The possibility that the rate of reductive elimination is slowed by binding of the nitrogen atom in **4** to the metal center appears less likely, given the fact that electron-poor N-aryl groups should disfavor N-coordination, but rates are slowest with these groups.

The effect of ligand electronic properties and bite angle on the rate of reductive elimination from **4** to **2** is also consistent with prior observations on the rates of C−C bond formation from Pd(II) complexes.[36,37] In our system complex **4s**, which bears a relatively electron poor ligand, undergoes reductive elimination 25 times faster than the related complex **4t**, which is ligated by a more electron-rich phosphine. This is likely due to the destabilizing effect of the electron-poor phosphine on the Pd(II) oxidation state.[36] The reductive elimination processes also appear to be most facile with wide-bite-angle ligands, which both destabilize the ground state of (P−P)Pd(Ar)(R) complexes and also stabilize the transition state for C−C bond formation.[37] The observed deuterium isotope effect at the carbon undergoing bond formation is consistent with rate-limiting C−C bond formation in the conversion of **4** to **2**, rather than rate-limiting phosphine dissociation.

Conclusions

In conclusion, our experiments on the conversion of (P−P)Pd(Ar)[N(Ar^1)(CH_2)$_3$CR=CHR′] complexes **3** to *N*-aryl-2-benzylpyrrolidine derivatives **2** indicate that the transformations proceed via syn insertion of the alkene into the Pd−N bond. This alkene *syn*-aminopalladation pathway has rarely been observed in well-characterized palladium complexes but plays a key role in catalytic reactions. These studies illustrate that ligand structure and heteroatom basicity/nucleophilicity[10] have a large impact on the rate of aminopalladation, and the observed trends could potentially be used in the design of new catalysts for reactions involving aminopalladation. Finally, our data suggest that insertion occurs from a four-coordinate alkene complex, rather than a five-coordinate species. This mechanistic information provides insight into previously observed trends in asymmetric Pd-catalyzed alkene carboamination reactions. Use of chiral bis-phosphine ligands provides poor enantioselectivity in these transformations,[11] which is likely due to dissociation of one arm of the bis-phosphine ligand prior to aminopalladation.

Experimental Section

In Situ Formation of Pd-Amido Complexes 3 and Conversion to 2. Representative Procedure. In a nitrogen-filled glovebox, (dppf)Pd(C_6H_4-*p*-F)(Br) (**5a**; 6.3 mg, 0.0075 mmol) and dppf (4.7 mg, 0.0085 mmol) were placed into a small vial. THF-d_8 (550 μL) was added, and the resulting orange solution was transferred to an NMR tube. 4-Fluorotoluene or 2-fluorotoluene (0.3 μL, 0.0027 mmol) was added as an internal ^{19}F standard, and the tube was sealed with a septum. The tube was cooled to −60 °C in the probe of an NMR spectrometer, and ^{1}H, ^{19}F, and ^{31}P spectra were obtained. A solution of potassium (4-fluorophenyl)(pent-4-enyl)amide (**6a**; 2.7 mg, 0.012 mmol) in 200 μL of THF-d_8 was prepared in the glovebox, and 121 μL (1 equiv) of that solution was loaded into a gastight syringe and injected into the NMR tube containing the Pd complex. The tube was inverted several times to ensure complete mixing, and a rapid color change from orange to red was observed. The tube was returned to the cold NMR probe and allowed to re-equilibrate at −60 °C, and a ^{19}F spectrum was obtained. The solution was then warmed to −20 °C and ^{1}H, ^{19}F, and ^{31}P spectra were obtained.

(dppf)Pd(C_6H_4-*p*-F)[N(C_6H_4-*p*-F)($CH_2CH_2CH_2CH$=CH_2)] (3a). ^{1}H NMR (400 MHz, THF-d_8): δ 7.95−7.87 (m, 4 H), 7.76

(36) (a) Ariafard, A.; Yates, B. F. *J. Organomet. Chem.* **2009**, *694*, 2075. (b) Ananikov, V. P.; Musaev, D. G.; Morokuma, K. *Eur. J. Inorg. Chem.* **2007**, 5390. (c) Hartwig, J. F. *Inorg. Chem.* **2007**, *46*, 1936.

(37) Zuidema, E.; van Leeuwen, P. W. N. M.; Bo, C. *Organometallics* **2005**, *24*, 3701.

(t, J = 8.6 Hz, 2 H), 7.59−7.40 (m, 10 H), 7.20−7.12 (m, 4 H), 7.06−7.01 (m, 2 H), 6.60 (q, J = 7.4 Hz, 2 H), 6.36 (t, J = 8.4 Hz, 2 H), 6.09 (t, J = 8.6 Hz, 2 H), 5.62 (tdd, J = 6.8, 10.0, 16.8 Hz, 1 H), 4.88−4.81 (m, 2 H), 2.57−2.51 (m, 1 H), 2.22−2.14 (m, 1 H), 1.70 (m, obscured by THF), 1.42−1.30 (m, 1 H), 1.20−1.08 (m, 1H). ^{19}F NMR (376 MHz, THF-d_8): δ −123.7 (m, Pd-C_6H_4F), −137.3 (s, N-C_6H_4F); ^{31}P NMR (162 MHz, THF-d_8): δ 24.9 (d, J = 38.1 Hz), 9.0 (d, J = 35.5 Hz).

The solution of the palladium−amido complex **3a** was warmed to 15 °C, with monitoring at 2 min intervals by ^{19}F spectroscopy for the appearance of peaks at −124.1 and −133.3 ppm (attributed to **4a**), along with diminishment of the peaks at −123.7 and −137.3 ppm. When the new peaks were near their maximum, the solution was cooled to −20 °C and ^{1}H, ^{19}F, and ^{31}P spectra were obtained. ^{19}F and ^{31}P data are reported; the ^{1}H spectrum for this and related compounds could not be extracted from the combined spectra of the species present in the reaction mixture.

(dppf)Pd(C_6H_4-*p*-F){CH_2[$CHCH_2CH_2CH_2N$(C_6H_4-*p*-F)]} (4a). ^{19}F NMR (376.9 MHz, THF-d_8): δ −124.1 (s), −133.3 (s). ^{31}P NMR (162 MHz, THF-d_8): δ 21.3 (d, J = 24.1 Hz), 16.6 (d, J = 21.7 Hz).

Synthesis of Authentic Samples of Pyrrolidine Products Formed in Kinetic Runs. Representative Procedure.[1a] Synthesis of 1-(4-Fluorophenyl)-2-(4-fluorobenzyl)pyrrolidine (2a). An oven- or flame-dried Schlenk tube was cooled under a stream of argon or nitrogen and charged with $Pd_2(dba)_3$ (2.6 mg, 2.8 μmol), dppf (3.1 mg, 5.6 μmol), NaO^{t}Bu (27 mg, 0.28 mmol), and 1-bromo-4-fluorobenzene (47 μL, 0.42 mmol). The tube was purged with argon or nitrogen, and a solution of 4-fluoro-*N*-(pent-4-enyl)aniline (51 mg, 0.28 mmol) in toluene (1 mL) was added. The mixture was heated to 80 °C with stirring until the starting material had been consumed, as judged by GC analysis (3 h). The reaction mixture was cooled to room temperature, quenched with saturated aqueous NH_4Cl (2 mL), and diluted with ethyl acetate (10 mL). The layers were separated, and the aqueous layer was extracted with ethyl acetate (2 × 10 mL). The combined organic extracts were dried over anhydrous sodium sulfate, filtered, and concentrated in vacuo. The crude product was then purified by flash chromatography on silica gel to afford 53 mg (68%) of the title compound as a colorless oil. ^{1}H NMR (400 MHz, $CDCl_3$): δ 7.19−7.11 (m, 2 H), 7.03−6.93 (m, 4 H), 6.60−6.53 (m, 2 H), 3.94−3.85 (m, 1 H), 3.42−3.32 (m, 1 H), 3.19−3.08 (m, 1 H), 2.94 (dd, J = 3.2, 13.6 Hz, 1 H), 2.58 (dd, J = 8.8, 13.6 Hz, 1 H), 1.95−1.74 (m, 4 H). ^{13}C NMR (100 MHz, $CDCl_3$): δ 161.8 (d, J = 245 Hz), 155.0 (d, J = 234 Hz), 143.9 (d, J = 1.6 Hz), 135.1 (d, J = 3.1 Hz), 130.9 (d, J = 7.6 Hz), 115.9 (d, J = 22.2 Hz), 115.4 (d, J = 20.7 Hz), 112.4 (d, J = 6.9 Hz), 60.2, 49.2, 38.0, 29.9, 23.4. ^{19}F NMR (376 MHz, $CDCl_3$): δ −117.0 (m), −130.7 (m). IR (film): 1225 cm^{-1}. MS (ESI): m/z 274.1413 (274.1407 calcd for $C_{17}H_{17}F_2N$, M + H$^+$).

Acknowledgment. We thank the National Science Foundation (Grant No. CHE-0705290) for financial support of this work. Additional funding was provided by GlaxoSmithKline, 3M, Amgen, and Eli Lilly. We also thank Pfizer for a generous gift of $Pd_2(dba)_3$. J.D.N. was supported by a GAANN fellowship.

Supporting Information Available: Text, tables, and figures giving experimental procedures, characterization data for all new compounds, copies of ^{1}H, ^{31}P, ^{19}F, and ^{13}C NMR spectra for selected compounds, and descriptions of stereochemical assignments. This material is available free of charge via the Internet at http://pubs.acs.org.